

# A Method for Inspecting Local Degradation in High-Current HTS Conductors Comprised of Stacked REBCO Tapes via Rotational Magnetization Measurement

Yuta Onodera , Naoki Hirano , Tomosumi Baba, and Toshiyuki Mito

**Abstract**—The structure of high-current-capacity high-temperature superconductor (HTS) conductors primarily comprise stacked REBCO tapes. During fabrication, degradation in critical current values has been observed. Although defect detection methods for individual REBCO tapes are well-established, equivalent methods for complete conductors remain under development. In this study, we utilized a rotational magnetization measurement technique to locate degradation within stacked REBCO tapes. To validate the principle of defect detection using this approach, we measured the magnetization of samples consisting of 10 layers of stacked REBCO tapes. The measurement yielded a magnetization signal with two peak values per rotation, demonstrating the potential for detailed defect analysis. Additionally, variations in the intensity and waveform of the magnetization signal were observed, correlating with the position of degraded REBCO tapes. These findings indicate that magnetization signal analysis can effectively pinpoint defect locations. The reliability of the magnetization signal was further corroborated through finite element method analysis.

**Index Terms**—HTS conductor, magnetization measurement, rotational magnetization measurement, stacked REBCO tapes.

## I. INTRODUCTION

THE structure of high-current-capacity HTS conductors primarily consists of stacked REBCO tapes [1], [2], [3]. The high-current-capacity HTS conductor currently being developed at the National Institute for Fusion Science features a unique configuration of alternating layers of REBCO tapes and pure aluminum sheets, all encased within an aluminum alloy jacket formed through friction stir welding [4]. During fabrication, it is essential to detect localized degradation within the conductor, which can result from localized shear stress or buckling stress, as illustrated in Fig. 1 [5]. To ensure quality and provide feedback on the production process, non-destructive and non-contact evaluation methods are required. Although defect detection methods

Received 25 September 2024; revised 11 November 2024 and 26 November 2024; accepted 2 December 2024. Date of publication 11 December 2024; date of current version 31 December 2024. This work was supported by the JSPS-KAKENHI under Grant 23K13086. (Corresponding author: Yuta Onodera.)

The authors are with the National Institute for Fusion Science (NIFS), National Institutes of Natural Sciences (NINS), Toki 509-5292, Japan (e-mail: onodera.yuta@nifs.ac.jp; hirano.naoki@nifs.ac.jp; baba.tomosumi@nifs.ac.jp; mito.toshiyuki@nifs.ac.jp).

Color versions of one or more figures in this article are available at <https://doi.org/10.1109/TASC.2024.3515961>.

Digital Object Identifier 10.1109/TASC.2024.3515961

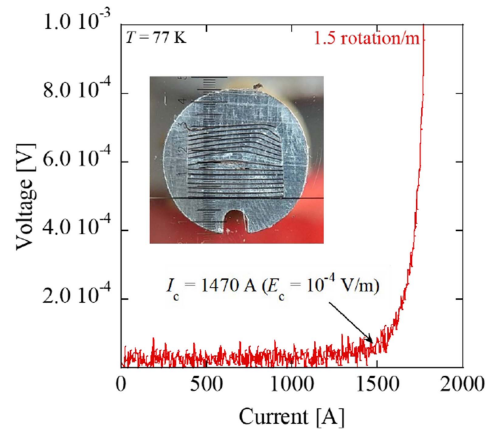


Fig. 1. Current-voltage characteristics of the compact FAIR conductor with 1.5 rotations per meter. The photograph shows the cross section of the compact FAIR conductor after fabrication of the first prototype [5], where buckling and folding are visible in the internal tapes.

for individual REBCO tapes are well-established [6], [7], [8], [9], [10], equivalent methods for the entire conductor are still in development. In this study, we applied a rotational magnetization measurement method to investigate degradation locations in stacked REBCO tapes. Typically, magnetization is measured by applying a magnetic field perpendicular to the tape surface. However, due to the monolithic structure of REBCO tape, aligning the external magnetic field parallel to the tape surface does not produce sufficient magnetization, as it fails to induce adequate shielding currents. Consequently, effective magnetization in a twisted conductor can be challenging, depending on the internal arrangement of the REBCO tapes. To address these limitations, we introduced an innovative approach involving the rotation of the REBCO tape within the magnetic field, in contrast to the conventional method of sweeping the external magnetic field.

## II. EXPERIMENT AND ANALYSIS

### A. Experimental Set Up

Fig. 2 illustrates the measurement mechanism [11]. The lower part of the shaft features a slit designed to hold stacked REBCO tape samples. A rotation stage, used for rotating the shaft, and

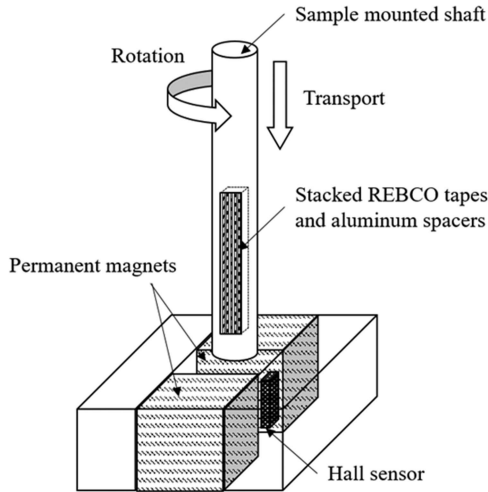


Fig. 2. Schematic diagram of the section where magnetization is measured during rotation and transport. The stacked REBCO tapes are magnetized by permanent magnets, and the magnetization signal is detected by a Hall sensor [11].

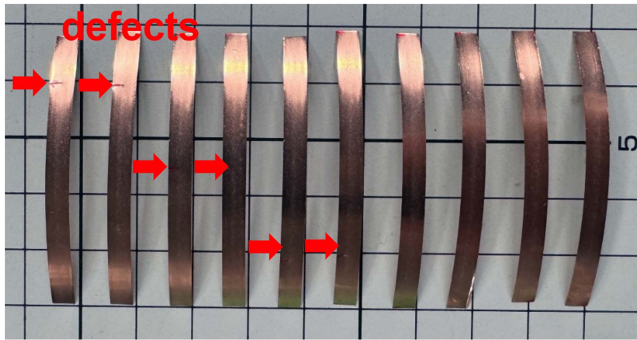


Fig. 3. Photograph of REBCO tapes before stacking, with intentionally introduced defects. The positions of the defects are indicated. The tapes were stacked from top to bottom, with aluminum spacers inserted between each layer. In the photograph, the bottom edge of the tapes is aligned at the 0 mm position.

a  $z$ -axis stage, for moving the shaft vertically, are mounted on the upper part of the shaft. As the shaft rotates and moves up and down, it passes between two permanent magnets, and the magnetization signal is measured using a Hall sensor (sensing area: 1.02 dia, sensitivity:  $0.55 \sim 1.1$  mV/kG, model BHT-921 by TOYO Corporation). The sensing direction of this Hall sensor is normal to the direction of the magnetic field. The entire measurement section is immersed in liquid nitrogen for cooling. The permanent magnets are cubic, each with a side length of 20 mm and a residual magnetization of 1.38 T. The magnets are positioned with a 9 mm gap between them, resulting in a central magnetic field of approximately 0.74 T where the shaft passes through.

The sample used in this study consisted of REBCO tapes (with a critical current  $I_c > 100$  A at 77 K in self-field, 4 mm in width, manufactured by Shanghai Superconductor Technology Co., Ltd.). Ten segments, each 50 mm in length, were prepared. As shown in Fig. 3, defects were intentionally introduced at half the width of the REBCO tapes. Specifically, six locations on the

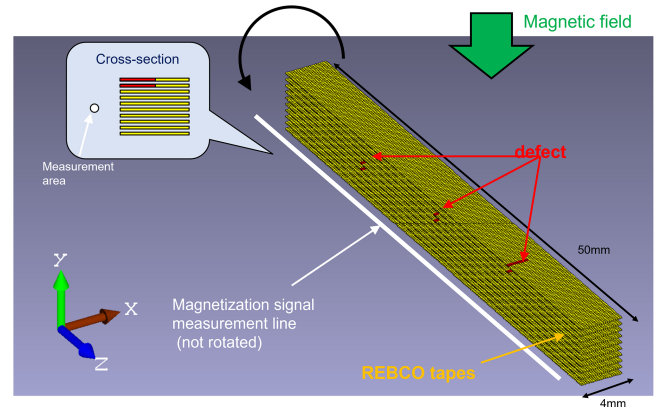


Fig. 4. Analytical model of 10 stacked REBCO tapes using the finite element method. The tapes have a length of 50 mm and a width of 4 mm. Defects are introduced in the red regions. The tapes were magnetized by rotating them in a static magnetic field, and the magnetic field signals were recorded along the white line, which corresponds to the position of the Hall sensor.

tapes were cut with scissors over half their width. Therefore, the critical current value is reduced by approximately half. The tapes were then stacked with 0.5 mm thick aluminum spacers placed between them to form the sample. The stacked samples were subsequently inserted into the slots at the end of the shaft, as shown in Fig. 2.

### B. Analytical Configuration

To validate the behavior of the rotational magnetization measurement, a finite element analysis was conducted. Using PHOTO-Series software, we modeled a 10-layer HTS tape stack, each layer being 0.1 mm thick, as illustrated in Fig. 4. Defects were introduced at the positions marked in red in Fig. 4, similar to those introduced in the tapes used in the experiments. The model was then rotated within a static magnetic field equivalent to that generated by the permanent magnets. The white line represents the magnetization signal measurement area, which remains stationary. This line corresponds to the distance between the Hall sensor and the sample, as shown in Fig. 2. The rotation is performed at approximately 4 seconds per rotation, consistent with the experiment, and the analysis considers the magnetic field history at each angular position. In the experiment, due to the time required for measurements, the effects of shielding currents from the aluminum enclosure and spacers are neglected. Additionally, to simplify the analysis, coupling currents in the aluminum components and the angular and magnitude dependence of the magnetic field on the critical current of the HTS conductors are not included. The  $n$ -value of the tape used in the simulation is set to 20.

## III. EXPERIMENTAL AND ANALYTICAL RESULTS

### A. Experimental Results

Fig. 5 shows the observed magnetization signal as the stacked sample was transported and rotated under a magnetic field. The  $x$ -axis represents the longitudinal displacement of the stacked tapes, the  $y$ -axis represents the rotation angle, and the  $z$ -axis

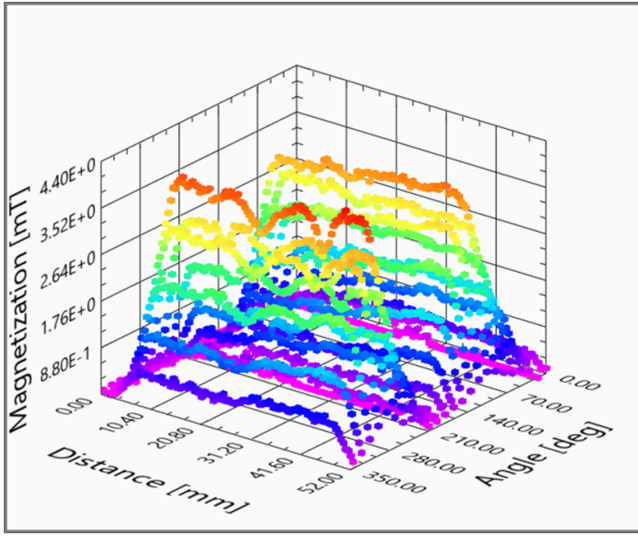


Fig. 5. Experimental results of the magnetic field distribution measured using the rotational magnetization method shown in Fig. 2.

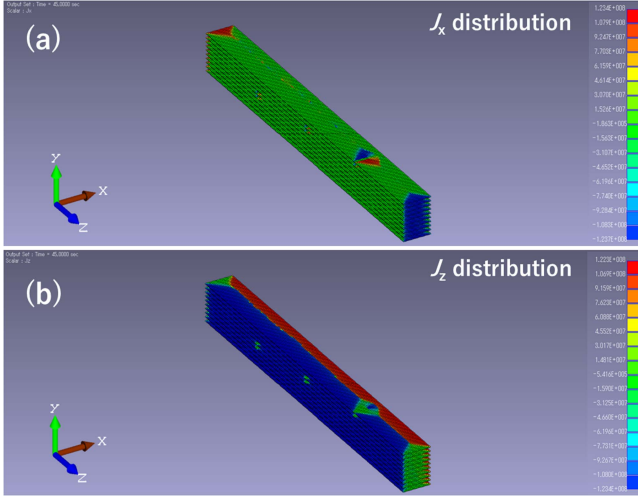


Fig. 6. Example results of current distribution analysis using the finite element method when the tape surface is parallel to the magnetic field: (a)  $J_x$  distribution and (b)  $J_z$  distribution.

represents the magnetic field detected by the Hall sensor. 0 degree indicates the position where the tape surface of the stacked tapes is parallel to the detection direction of the Hall sensor. The measurement involved rotating the sample through 360 degrees in 15-degree increments, with a longitudinal displacement of 0.2 mm for each step. This procedure allowed for continuous measurement of the signal waveform with two peak values along the length of the stacked REBCO tapes. It was also observed that the signal behavior changed in the regions where degradation was present.

### B. Analytical Results

Fig. 6 shows the analytical results of the current distribution on the tape surface when the magnetic field is parallel to the tape

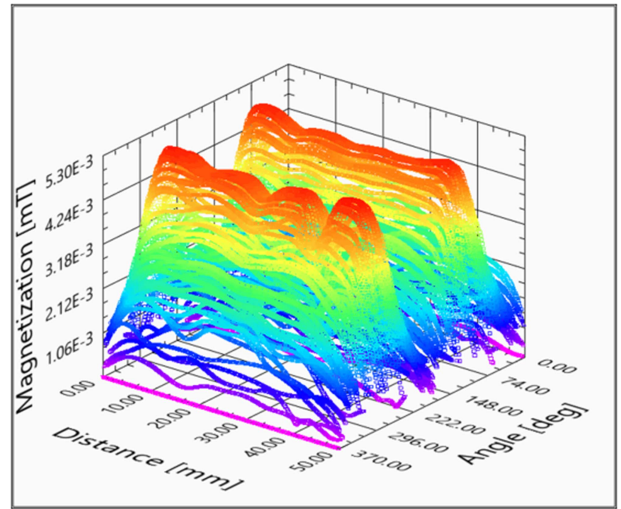


Fig. 7. Finite element analysis results of the magnetic field distribution. The magnetization signal is derived along the measurement line shown in Fig. 4 during magnetization under rotation.

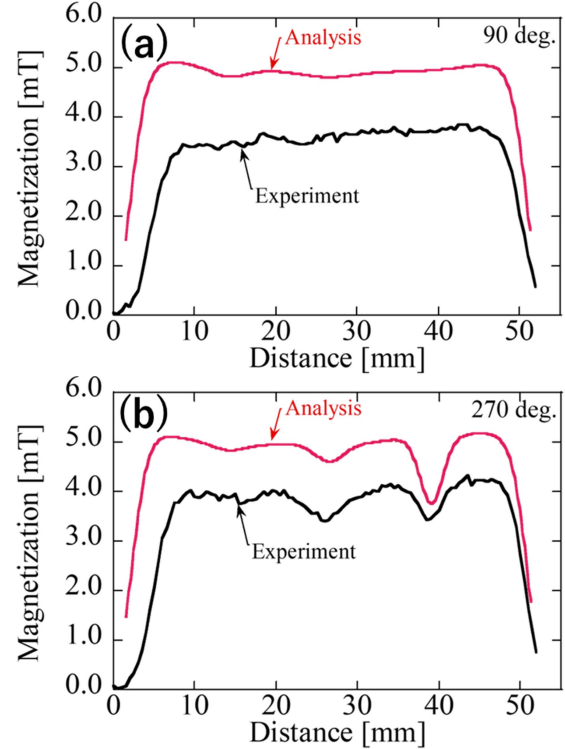


Fig. 8. Comparison of experimental and analytical results for the magnetization signal distribution at peak values for rotations of (a) 90 degrees and (b) 270 degrees. The values analyzed are shifted according to the position of the distance transported during the experiment.

surface at 90-degree position. Fig. 6(a) depicts the current distribution along the  $x$ -axis, representing the tape's width direction, while Fig. 6(b) shows the current distribution along the  $z$ -axis, representing the longitudinal direction. The color map indicates the direction of the current. The combined results from both figures demonstrate that shielding currents are induced in the 10-layer stacked REBCO tapes.

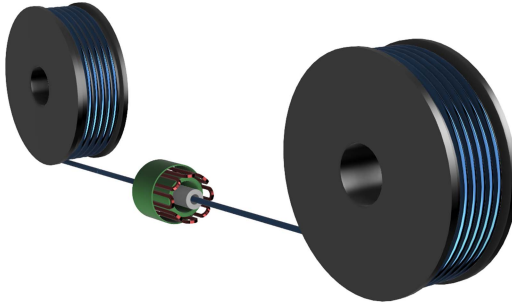


Fig. 9. Schematic diagram of the measurement setup for long conductors. A reel-to-reel system is employed, with superconducting coil windings generating the rotating magnetic field.

Fig. 7 shows the calculated magnetic field distribution along the measurement line indicated in Fig. 4, for one full rotation in a static magnetic field. The  $x$ -axis represents the longitudinal distance, the  $y$ -axis represents the rotation angle, and the  $z$ -axis represents the magnetization signal. The magnetization signal varies depending on the position of the defects, indicating that this method can be used to evaluate the locations of defects.

#### IV. DISCUSSION

Fig. 8 shows the peak values of the signals at 90 degrees and 270 degrees, extracted from Figs. 5 and 7, respectively. It can be observed that the analytical results are consistent with the experimental findings. Specifically, the defect locations are at 12 mm, 28 mm, and 40 mm in Fig. 8, where a decay in the magnetization signal is observed in both experimental and analytical values at the defective sections. This consistency indicates that the signal strength varies with the depth of the degradation position. It is clear that the magnetization signal varies with the distance between the defect position and the Hall sensor, and that the depth of the defect position can also be determined by comparing the two peak values.

#### V. SUMMARY

A method for detecting degradation locations in stacked 10-layer REBCO tapes using magnetization measurements was investigated, with defects intentionally introduced into the tapes. The intensity distribution of the magnetization signal shows a decrease at the degraded positions. A comparison of analytical and experimental results confirms that the signal strength varies with the depth of degradation. The degradation locations in the

stacked 10-layer REBCO tapes can be identified by analyzing the rotational magnetization measurements. The observational limits regarding the number of layers and defect shapes will be examined in future studies. Furthermore, future applications for long conductors are under consideration, particularly in relation to a short conductor evaluation system currently in development. Additionally, we are exploring the feasibility of a reel-to-reel system for longer lengths, as rotating all HTS conductors presents challenges. In this system, a rotating magnetic field generator using superconducting wires, similar to stator windings, will be necessary, as shown in Fig. 9.

#### REFERENCES

- [1] D. C. van der Laan, D. J. Weiss, and M. D. McRae, "Status of CORC cables and wires for use in high-field magnets and power systems a decade after their introduction," *Supercond. Sci. Technol.*, vol. 32, no. 3, Feb. 2019, Art. no. 033001, doi: [10.1088/1361-6668/aafc82](https://doi.org/10.1088/1361-6668/aafc82).
- [2] M. J. Wolf, C. M. Bayer, W. H. Fietz, R. Heller, S. I. Schlachter, and K.-P. Weiss, "Toward a high-current conductor made of HTS crossconductor strands," *IEEE Trans. Appl. Supercond.*, vol. 26, no. 4, Jun. 2016, Art. no. 4801504, doi: [10.1109/TASC.2016.2525734](https://doi.org/10.1109/TASC.2016.2525734).
- [3] M. Takayasu, L. Chiesa, P. D. Noyes, and J. V. Minervini, "Investigation of HTS twisted stacked-tape cable (TSTC) conductor for high-field, high-current fusion magnets," *IEEE Trans. Appl. Supercond.*, vol. 27, no. 4, Jun. 2017, Art. no. 6900105, doi: [10.1109/TASC.2017.2652328](https://doi.org/10.1109/TASC.2017.2652328).
- [4] T. Mito et al., "Improvement of  $I_c$  degradation of HTS conductor (FAIR conductor) and FAIR coil structure for fusion device," *IEEE Trans. Appl. Supercond.*, vol. 31, no. 5, Aug. 2021, Art. no. 4202505, doi: [10.1109/TASC.2021.3069923](https://doi.org/10.1109/TASC.2021.3069923).
- [5] Y. Onodera, N. Hirano, T. Baba, T. Mito, and R. Kawanami, "Development of a compact HTS-FAIR conductor for magnet application," *IEEE Trans. Appl. Supercond.*, vol. 33, no. 5, Aug. 2023, Art. no. 4801004, doi: [10.1109/TASC.2023.3254492](https://doi.org/10.1109/TASC.2023.3254492).
- [6] S. Furtnar et al., "Reel-to-reel critical current measurement of coated conductors," *Supercond. Sci. Technol.*, vol. 17, no. 5, Mar. 2004, Art. no. S281, doi: [10.1088/0953-2048/17/5/037](https://doi.org/10.1088/0953-2048/17/5/037).
- [7] K. Higashikawa et al., "High-speed scanning hall-probe microscopy for two-dimensional characterization of local critical current density in long-length coated conductor," *Phys. Procedia*, vol. 27, pp. 228–231, 2012, doi: [10.1016/j.phpro.2012.03.452](https://doi.org/10.1016/j.phpro.2012.03.452).
- [8] S. Zou, C. Gu, T. Qu, S. Chen, X. Li, and Z. Han, "Examination and analysis of critical current uniformity of long HTS tapes by the MCorder," *IEEE Trans. Appl. Supercond.*, vol. 25, no. 3, Jun. 2015, Art. no. 8801005, doi: [10.1109/TASC.2014.2374418](https://doi.org/10.1109/TASC.2014.2374418).
- [9] X. Hu et al., "An experimental and analytical study of periodic and aperiodic fluctuations in the critical current of long coated conductors," *IEEE Trans. Appl. Supercond.*, vol. 27, no. 4, Jun. 2017, Art. no. 9000205, doi: [10.1109/TASC.2016.2637330](https://doi.org/10.1109/TASC.2016.2637330).
- [10] Y. Li, S. Chen, M. Paidipilli, R. Jain, C. Goel, and V. Selvamanickam, "A reel-to-reel scanning Hall problem microscope for characterizing long REBCO conductor in magnetic fields up to 5 tesla," *IEEE Trans. Appl. Supercond.*, vol. 32, no. 4, Jun. 2022, Art. no. 9000206, doi: [10.1109/TASC.2022.3140688](https://doi.org/10.1109/TASC.2022.3140688).
- [11] Y. Onodera et al., "Rotating magnetization method for inspection of local defect in HTS conductor," *J. Phys.: Conf. Ser.*, vol. 1857, 2021, Art. no. 012012, doi: [10.1088/1742-6596/1857/1/012012](https://doi.org/10.1088/1742-6596/1857/1/012012).